

# Growth History and Significant Events of Cerebral Aneurysm with Fluid-Structure Interaction Simulations

Jozsef Nagy<sup>1</sup>, Julia Maier<sup>2</sup>, Wolfgang Fenz<sup>3</sup>, Zoltan Major<sup>2</sup>, Andreas Gruber<sup>4</sup>, Matthias Gmeiner<sup>4</sup>

<sup>1</sup>eulerian-solutions e.U.

Leonfeldnerstraße 245, Linz, Austria

jozsef.nagy@eulrian.solutions.com

<sup>2</sup>Johannes Kepler University Linz - Institute of Polymer Product Engineering

Altenberger Strasse 69, Linz, Austria

julia.maier@jku.at; zoltan.major@jku.at

<sup>3</sup>RISC Software GmbH

Softwarepark 32a, Hagenberg, Austria

[wolfgang.fenz@risc-software.at](mailto:wolfgang.fenz@risc-software.at)

<sup>4</sup>Johannes Kepler University Linz - Universitätsklinik für Neurochirurgie

Wagner-Jauregg-Weg 15, Linz, Austria

andreas.gruber\_1@kepleruniklinikum.at; matthias.gmeiner@kepleruniklinikum.at

**Abstract** - We analyzed the growth process of a single cerebral aneurysm using Fluid-Structure Interaction (FSI) simulations establishing a history including important events in morphology, hemodynamics as well as structural mechanics.

Data of one patient was obtained between the years 2012 and 2022. The medical imaging data of these aneurysms was provided in the form of digital subtraction angiography, which was transformed into stereolithography format as geometry input. With the FSI simulations typical hemodynamic (wall shear stress, oscillatory shear index) and a structural mechanic quantity (Mises stress) were identified. With the addition of morphological parameters (Size, Volume, L2-norm of Gaussian curvature) significant changes can be found during the growth history of the selected aneurysm.

Wall shear stress is highest during aneurysm initiation, while decreasing during aneurysm growth. Oscillatory shear index increases over time especially in the region of strong aneurysm growth. Strong changes in geometry induce subsequent changes in hemodynamics. Wall stress remains constant throughout the growth period of the selected aneurysm. However, shortly before aneurysm rupture wall stress increases significantly.

Simulation results of aneurysm growth history can be utilized to identify important events of a growing aneurysm, enabling a better understanding of the behaviour as well as a better estimation for the best time for patient treatment.

**Keywords:** cerebral aneurysms, growth history, Fluid-Structure Interaction, aneurysm initiation, aneurysm rupture

## 1. Introduction

Cerebral aneurysms occur in approximately 2-5% of the general population [1]. Rupture of aneurysms leads to subarachnoid hemorrhage (SAH), which is usually associated with high mortality and morbidity. Several studies have highlighted different clinical, genetic, morphological or hemodynamic factors known in the development, growth and rupture of cerebral aneurysms [2-4].

The increasing utilization of medical imaging has led to the detection of a greater number of unruptured aneurysms. This, in turn, leads to a greater need for treatment decisions. Only aneurysms close to rupture should be treated, because the treatment itself carries many risks for the patient. Therefore, reliable decision support is needed to better treat patients.

Multiple studies in literature using computational fluid dynamics (CFD) have been able to demonstrate significantly different hemodynamics between ruptured and unruptured aneurysms [5-7]. Hemodynamic phenomena provide mechanical triggers that translate into biological signals that lead to eventual aneurysm growth and rupture [8]. Hemodynamics is influenced by the geometry of the aneurysm, therefore also the morphological parameters [9].

Furthermore, although many detailed fluid dynamics simulations, including complex flow models, have already been performed [2,3,5-10], only a few have been done so far studies focused on structural dynamics calculations. [11,12]. Previously we published a comprehensive assessment of a method using fluid-structure interaction (FSI) analysis, which was validated with the help of an experimental setup [13].

With this method it is possible to track the development of cerebral aneurysms and quantitatively analyze the change in aneurysm behaviour between the medical imaging data from two subsequent routine examinations.

## 2. Methods

### 2.1. Patient image data and simulation geometry

As discussed in more detail in [13] the aneurysm geometry is extracted from medical image data obtained via digital subtraction angiography (DSA). Intensity thresholding and minor editing of the voxel volume is performed in the segmentation of the cerebral aneurysm geometry. This is converted into a surface mesh and inlet as well as outlet planes are placed. The final set of surfaces (vessel, aneurysm, inflow, outflow) is saved as STL files. The volumetric fluid mesh is automatically generated utilizing the STL files as input. The solid vessel wall mesh is extruded from the fluid mesh with a certain pre-defined thickness (0.2 mm).

For this study a set of medical imaging data of the same patient from the years 2012, 2013, 2017, 2018, 2020 and 2022 (see figure 1) is analyzed and changes in morphology, hemodynamic and structural mechanics identified. Before the image in 2022 SAH occurred in the aneurysm.

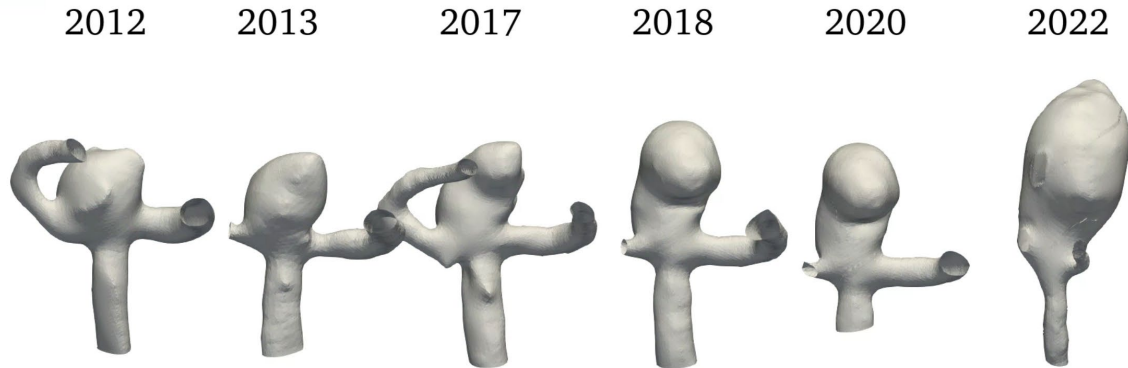


Fig. 1: Geometries extracted from medical imaging data; date of data indicated in the top

### 2.2. Hemodynamic and structural mechanic modelling

An in-house finite volume solver [13] based on the open-source computational fluid dynamics tool OpenFOAM [14] in combination with the fluid-structure interaction library solids4Foam [15] was used to numerically solve the unsteady equations of the process.

For hemodynamic modelling the governing equations are given by the principles of mass and momentum conservation with the help of the continuity equation as well as the Navier Stokes equations,

$$\frac{\partial \rho}{\partial t} + \nabla \cdot \rho \mathbf{u} = 0 \quad (1)$$

$$\frac{\partial \rho \mathbf{u}}{\partial t} + \nabla \cdot \rho \mathbf{u} \mathbf{u} = -\nabla p + \nabla \cdot \boldsymbol{\sigma} + \mathbf{F} \quad (2)$$

Here,  $\rho$  is the fluid density,  $t$  is the time,  $\mathbf{u}$  is the velocity vector,  $p$  is the fluid pressure,  $\boldsymbol{\sigma}$  is the fluid stress tensor and  $\mathbf{F}$  is the vector of possibly additional forces (e.g. gravitation). In order to analyse hemodynamic results, the oscillatory shear index is defined as

$$OSI = \frac{1}{2} \left( 1 - \frac{\left\| \int_0^T \boldsymbol{\sigma}_w dt \right\|}{\int_0^T \|\boldsymbol{\sigma}_w\| dt} \right) \quad (3)$$

where,  $\sigma_s$  is the fluid wall shear stress (WSS) vector. The index is defined in the interval between [0;0.5] and gives the quantity of oscillatory behaviour of the wall shear stress on the fluid wall.

For structural mechanic modelling, the principle of force conservation is utilized. For linear elastic materials the equation is given by

$$\int_{\Omega_0} \frac{\partial^2 \rho_s \mathbf{u}_s}{\partial t^2} d\Omega_0 = \oint_{\Gamma_0} \mathbf{n}_0 \cdot \boldsymbol{\sigma}_s d\Gamma_0 + \int_{\Omega_0} \rho_s \mathbf{b} d\Omega_0 \quad (3)$$

$$\boldsymbol{\sigma}_s = 2\mu \boldsymbol{\varepsilon}_s + \lambda \text{tr}(\boldsymbol{\varepsilon}_s) \mathbf{I} \quad (4)$$

$$\boldsymbol{\varepsilon}_s = \frac{1}{2} (\nabla \mathbf{u}_s + \nabla \mathbf{u}_s^T) \quad (5)$$

$$\mu = \frac{E}{2(1 + \nu)} \quad (6)$$

$$\lambda = \frac{\nu E}{(1 + \nu)(1 - 2\nu)} \quad (7)$$

Here,  $\rho_s$  is the solid density,  $\mathbf{u}_s$  is the vector of displacement,  $\mathbf{n}_0$  is the surface normal vector,  $\boldsymbol{\sigma}_s$  is the solid stress tensor and  $\mathbf{b}$  is the vector of possible body forces.  $E$  is Young's modulus and  $\nu$  is Poisson's ratio.

Equations (1)-(7) are coupled iteratively in a Fluid-Structure Interaction method described in further detail in [13].

### 3. Discussion

For the aneurysm initiation and growth process, the role of the wall shear stress as well as OSI has recently been discussed with divergent results [3,16]. Typically, they show an inverse behaviour during aneurysm growth, while one is increasing, the other is decreasing. Some studies [11,12] do incorporate structural mechanic analysis into the behaviour of aneurysms, however these mostly concentrate on abdominal aneurysms. According to the knowledge of the authors, almost no work was done on the structural mechanic analysis of cerebral aneurysms.

For best visualization wall shear stress will be shown in an interval between 0 and 1 Pa, OSI between 0 and 0.25 and the Mises stress of the vessel wall between 0 and 1.2 kPa.

Figure 1 (a) shows the change in wall shear stress (WSS) in Pa over the years. During the first year a significant region with high WSS values can be identified. This correlates to the initiation process of the aneurysm as described in [3,16]. WSS gradually is being reduced in the aneurysm during the growth process. Figure 1 (b) shows the development of OSI in the aneurysm. While being comparatively low during the initiation process, a clear region of increased OSI can be identified in the direction of growth during the years. Figure 1 (c) shows the Mises stress in the vessel wall. No significant qualitative change can be identified especially in the early stages of the growth, which implies that aneurysm growth in the initial stages did not change the stress on the vessel tissue.

Table 1: Change in typical parameters of the investigated aneurysm over the years

Parameter	2012	2013	2017	2018	2020	2022
S [mm]	6.3	6.3	6.7	7.9	7.8	9.9
V [mm <sup>3</sup> ]	132	134	157	259	249	505
GLN [-]	1.92	1.60	3.54	2.57	2.70	4.70
WSS <sub>av</sub> [Pa]	0.322	0.232	0.147	0.117	0.1	0.149
OSI <sub>av</sub> [-]	0.023	0.024	0.030	0.053	0.056	0.210
MISES <sub>av</sub> [Pa]	0.79e5	0.80e5	0.79e5	0.79e5	0.93e5	0.97e5

Table 1 shows the investigated parameters (morphologic: Size S, Volume V, L2 norm of Gaussian curvature; hemodynamic: average WSS and average OSI; structural mechanic: average Mises stress). Here, the average values are taken only from the aneurysm, not the parent vessel. Additionally, the evaluation of maximum values is omitted as they are restricted to local positions in the aneurysm and are not adequate for analyzing the overall behaviour of the aneurysm.

During the initial years of 2012 and 2013 the morphology of the aneurysm did not change considerably, WSS decreased indicating the end of aneurysm initiation and a transition into a dynamic growths period. The mean stress in the wall did not change in this year.

In the next period until 2017 the most significant change occurred in the morphology of the aneurysm. The top right section in figures 1 and 2 of the aneurysm in 2017 shows significant growth in a given direction. This growth not only increases the volume, but also the curvature of the aneurysm. Additional decrease in WSS and a small increase in OSI can be seen, while the wall stress remains constant.

Within a single year until 2018 significant changes can be observed in the behaviour of the aneurysm. The previous growth direction changes and the volume increases significantly by 65% withing one year. WSS decreases and a significant increase in OSI (~77%) can be observed especially in the region of aneurysm growth. This corresponds to findings in [3,16]. Still wall stress remains constant during this strong growth period.

In the next period until 2020 morphology and hemodynamics do not change considerably, however the wall vessel stress increases unexpectedly by ~18% after being constant throughout the previous 6 years.

In the last period between 2020 and 2022 SAH occurred in the aneurysm changing the morphology. OSI increases by ~375%, while WSS and Mises stress increase by 49% and 4% respectively.

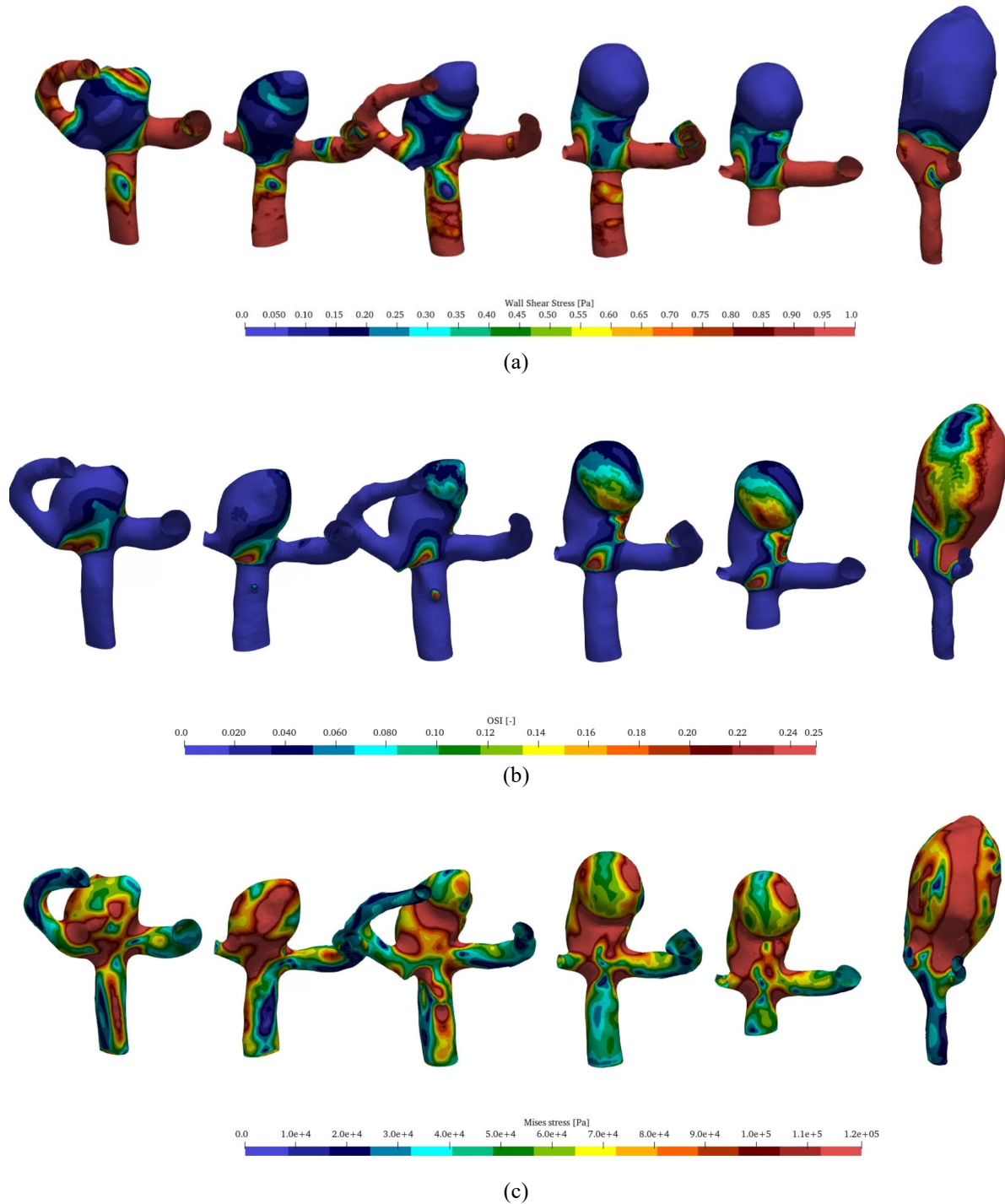


Fig. 2: Wall shear stress (a), oscillatory shear index (OSI; b) and Mises stress (c) in the investigated geometries

The evaluation of aneurysm history clearly shows significant events during the years:

1. High WSS region during aneurysm initiation and slow decrease of WSS during aneurysm growth
2. Increase of OSI (especially in the direction of aneurysm growth) over the years.
3. Abrupt changes in geometry induce subsequent changes in hemodynamics implying unfavourable growth.
4. Due to increased unfavourable growth wall stress is creased in the years before SAH, while wall stress remains constant in the initial period of growth.

#### 4. Conclusion

The evaluation of aneurysm growth history can be a valuable tool in the hands of neurosurgeons. With the ARES Software Suite [13] medical personnel without simulation knowledge can conduct FSI simulations on multiple aneurysms establishing the patient history. Significant changes in morphology, hemodynamics and structural mechanics can indicate certain periods of aneurysm growth and can be used to better estimate the best time for patient treatment.

In future steps, more parameters will be included into evaluation as well as the patient pool will be increased to identify typical events during the growth of cerebral aneurysms.

#### Acknowledgements

This work was supported by research subsidies granted by the government of Upper Austria via the FFG (Austrian Research Promotion Agency) [grant number 872604 (Project MEDUSA) as well as grant number FO999895610 (Project ARES)]. RISC Software GmbH is Member of UAR (Upper Austrian Research) Innovation Network.

This study was approved by the local ethics committee (Ethikkommission der medizinischen Fakultät der Johannes Kepler Universität; EK Nr: 1129/2022), and the requirement for acquisition of informed consent from patients was waived owing to the retrospective nature of the research.

#### References

- [1] S. Dhar, M. Tremmel, J. Mocco, M. Kim, J. Yamasolo, A. H. Siddiqui, L. N. Hopkins and H. Meng, “Morphology Parameters for Aneurysm Rupture Risk Assessment” *Neurosurgery*, vol. 63, no. 2, pp. 185-197, 2008.
- [2] S. Jirjees, Z. M. Htun, I. Aldawudi, P. C. Patwal and S. Khan, “Role of Morphological and Hemodynamic Factors in Predicting Intracranial Aneurysm Rupture: A Review” *Cureus*, vol. 12, no. 7: e9178, 2020.
- [3] H. Meng, V.M. Tutino, J. Xiang, and A. Siddiqui: “High WSS or Low WSS? Complex Interactions of Hemodynamics with Intracranial Aneurysm Initiation, Growth, and Rupture: Toward a Unifying Hypothesis” *AJNR Am. J. Neuroradiol.*, vol. 35, no. 7, pp. 1254-1262, 2014.
- [4] Japan Investigators UCAS, A. Morita, T. Kirino, K. Hashi, N. Aoki, S. Fukuhara, N. Hashimoto, T. Nakayama, M. Sakai, A. Teramoto, S. Tominari and T. Yoshimoto, “The natural course of unruptured cerebral aneurysms in a Japanese cohort”. *N Engl J Med*, vol. 366, pp. 2474- 2482, 2012.
- [5] P. Jiang, Q. Liu, J. Wu, X. Chen, M. Li, Z. Li, S. Yang, R. Guo, B. Gao, Y. Cao and S. Wang, “A Novel Scoring System for Rupture Risk Stratification of Intracranial Aneurysms: A Hemodynamic and Morphological Study”. *Front. Neurosci.* vol. 12, no. 596, 2018.
- [6] F.J. Detmer, B.J. Chung, F. Mut, M. Slawski, F. Hamzei-Sichani, C. Putman, C. Jimenez and J.R. Cebral, “Development and internal validation of an aneurysm rupture probability model based on patient characteristics and aneurysm location, morphology, and hemodynamics”. *Int J CARS*, vol. 13, pp. 1767–1779, 2018.
- [7] F.J. Detmer, B.J. Chung, F. Mut, M. Slawski, F. Hamzei-Sichani, C. Putman, C. Jimenez and J.R. Cebral, “Development of a statistical model for discrimination of rupture status in posterior communicating artery aneurysms”. *Acta Neurochir*, vol. 160, pp. 1643–1652, 2018.

- [8] S. Soldozy, P. Norat, M. Elsarrag, A. Chatrath, J.S. Costello, J.D. Sokolowski, P. Tvrđik, M.Y.S. Kalani and M.S. Park. “The biophysical role of hemodynamics in the pathogenesis of cerebral aneurysm formation and rupture”. *Neurosurg Focus*. Vol. 47, no. 1, pp. E11. 2019.
- [9] J. M. Acosta, A. F. Cayron, N. Dupuy, G. Pelli, B. Foglia, J. Haemmerli, E. Allermann, P. Bijlenga, B. R. Kwak and S. Morel, “Effect of Aneurysm and Patient Characteristics on Intracranial Aneurysm Wall Thickness”, *FRONT CARDIOVASC MED*, vol. 8, Article 775307, 2021
- [10] J.R. Cebral, F. Mut, D. Sforza, R. Löhner, E. Scrivano, P. Lylyk, C. Putman, “Clinical application of image-based CFD for cerebral aneurysms”. *Int. j. numer. method. biomed. eng.*, vol. 27, pp. 977–992, 2011.
- [11] T.C. Gasser, M. Auer, F. Labruto, J. Swedenborg, J. Roy, „Biomechanical rupture risk assessment of abdominal aortic aneurysms: Model complexity versus predictability of finite element simulations”. *Eur. J. Vasc. Endovasc. Surg.*, vol. 40, pp. 176–185, 2010.
- [12] C. Reeps, M. Gee, A. Maier, M. Gurdan, H.H. Eckstein and W.A. Wall, “The impact of model assumptions on results of computational mechanics in abdominal aortic aneurysm”, *J. Vasc. Surg.*, vol. 51, pp. 679–688, 2010.
- [13] J. Nagy, J. Maier, V. Miron, W. Fenz, Z. Major, A. Gruber and M. Gmeiner, “Methods, Validation and Clinical Implementation of a Simulation Method of Cerebral Aneurysms”, *JBEb*, vol. 10, pp. 10-19, 2023, DOI: 10.11159/jbeb.2023.003
- [14] H.G. Weller, G. Tabor, H. Jasak, and C. Fureby, “A tensorial approach to computational continuum mechanics using object orientated techniques”, *Comput. phys.*, vol. 12, no. 6, pp. 620 – 631, 1998.
- [15] P. Cardiff, A. Karač, P. De Jaeger, H. Jasak, J. Nagy, A. Ivanković and Ž. Tuković, “An open-source finite volume toolbox for solid mechanics and fluid-solid interaction simulations”, arXiv:1808.10736v2, 2018, available at <https://arxiv.org/abs/1808.10736>
- [16] S. Fujimura, K. Tanaka, H. Takao, T. Okudaira, H. Koseki, A. Hasebe, T. Suzuki, Y. Uchiyama, T. Ishibashi, K. Otani, K. Karagiozov, K. Fukudome, M. Hayakawa, M. Yamamoto and Y. Murayama, “Computational fluid dynamic analysis of the initiation of cerebral aneurysms”, *J Neurosurg*, vol. 137, pp. 335–343, 2022.